

Geophysical Research Letters

RESEARCH LETTER

10.1029/2019GL086058

Key Points:

- The unevenness of tropical rainfall increases with warming because of Clausius-Clapeyron scaling of subcloud moist static energy
- Circulation changes can increase or decrease rainfall locally, but the total effect is a decrease in the area of active convection
- The area of active convection will decrease even with uniform warming

Supporting Information:

- Supporting Information S1
- Figure S1
- Figure S2

Correspondence to:

Y. Zhang
yz8@princeton.edu

Citation:

Zhang Y., & Fueglistaler, S. (2019). Mechanism for increasing tropical rainfall unevenness with global warming. *Geophysical Research Letters*, 46, 14,836–14,843. <https://doi.org/10.1029/2019GL086058>

Received 30 OCT 2019

Accepted 28 NOV 2019

Accepted article online 4 DEC 2019

Published online 21 DEC 2019

Corrected 5 OCT 2020

This article was corrected on 5 OCT 2020. See the end of the full text for details.

©2019. American Geophysical Union.
All Rights Reserved.

Mechanism for Increasing Tropical Rainfall Unevenness With Global Warming

Yi Zhang¹ and Stephan Fueglistaler^{1,2}

¹Program in Atmospheric and Oceanic Sciences, Princeton University, Princeton, NJ, USA, ²Department of Geosciences, Princeton University, Princeton, NJ, USA

Abstract Global climate models predict that tropical rainfall will be distributed more unevenly with global warming; that is, dry regions or months will get drier and wet regions or months will get wetter. Previous mechanisms such as “dry-get-drier, wet-get-wetter”; “rich-get-richer”; or “upped-ante” focus on the spatial pattern of rainfall changes rather than the changes in probability distribution. Here, we present a quantitative explanation of the warming-induced probability distribution change of rainfall: Subcloud moist static energy (MSE) gradients are amplified by Clausius-Clapeyron relationship given roughly uniform warming and constant relative humidity. Therefore, the present-day wet regions will become more competitive for convection in a warmer world. Though changes in the atmospheric circulation pattern can enhance rainfall in one place and suppress rainfall in another, our results show that the total effect should be a decrease in the area of active convection even with uniform warming.

Plain Language Summary Tropical rainfall on average increases with global warming. However, dry regions experience rainfall reductions, while wet regions receive even more rain. This is due to the thermodynamic exponential dependence of moisture on temperature. With the same amount of warming, wet regions experience larger increase in moisture than dry regions and therefore become even more competitive for convection in a warmer world.

1. Introduction

Tropical rainfall falls very unevenly in space. Figure 1(a) shows that three quarters of the total rainfall falls on only a quarter of surface area when the observed monthly mean rainfall intensities from Tropical Rainfall Measuring Mission (TRMM) (Huffman et al., 2007) are sorted in ascending order. In the context of global warming, climate models predict enhancement of rainfall unevenness with increasing temperature (Giorgi et al., 2011; Lintner et al., 2012; Liu & Allan, 2013; Polson & Hegerl, 2017), which has implications for drought and flood projection and water resource management (Lintner et al., 2012). The unevenness of rainfall distribution is usually measured with the rainfall differences between the “wet” and the “dry” regions defined as, for example, the upper portion and the lower portion of rainfall intensity (Allan et al., 2010; Gu & Adler, 2018; Liu & Allan, 2013; Polson et al., 2013; Polson & Hegerl, 2017), the local wettest and driest month of a year (Chou et al., 2013; Chou & Lan, 2012), and the frequency of rainfall above and below some thresholds (Lintner et al., 2012). Despite the variety of metrics, the unevenness of rainfall is robustly projected to rise, and this signal is emerging in the observational records (Allan et al., 2010; Chou & Lan, 2012; Gu & Adler, 2018; Liu & Allan, 2013; Polson & Hegerl, 2017).

Often cited in support of the strengthening contrast between wet and dry regions or seasons with global warming is the rainfall change mechanisms (e.g. Lintner et al., 2012) such as the “dry-get-drier, wet-get-wetter” mechanism (Held & Soden, 2006); the “upped-ante” mechanism (Neelin et al., 2003); or the “rich-get-richer” mechanism (Chou & Neelin, 2004). These mechanisms aim at explaining certain features of rainfall change, which we will briefly summarize below, but none of them directly addresses the change in the unevenness. The mechanisms predicting future rainfall change usually make use of two approximations: (i) The relative humidity in the boundary-layer remains constant for energetic reasons (Held & Soden, 2000), so that the boundary-layer moisture increases by 7%/K following the Clausius-Clapeyron relationship. (ii) The large-scale circulation pattern remains unchanged. The combination of these two approximations together with the assumption that changes in surface temperature gradients are small

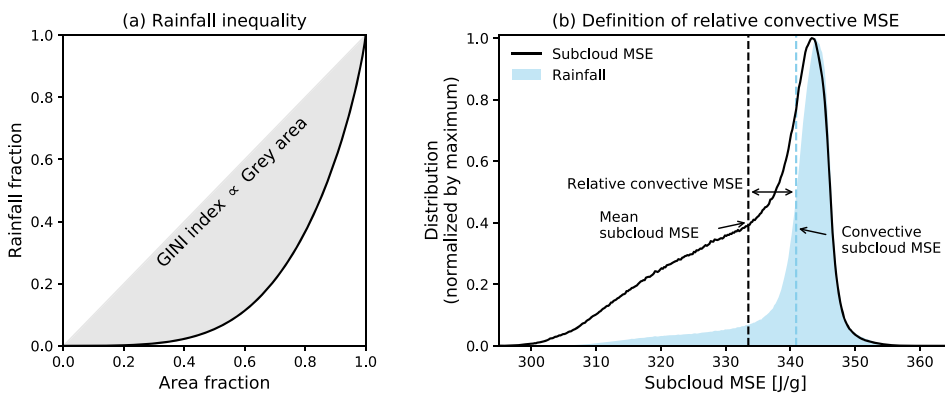


Figure 1. (a) Schematic of the Gini index. Cumulative rainfall fraction as a function of cumulative area fraction with rainfall intensity sorted in ascending order. (b) Schematic of the relative convective MSE.

results in the amplification of moisture convergence or divergence by 7%/K with warming, leading to the amplification of the precipitation-minus-evaporation pattern by the same amount. This mechanism, widely known as “dry-get-drier, wet-get-wetter,” accurately captures the climatological zonal-mean precipitation-minus-evaporation changes across all latitudes, yet its utility in explaining rainfall changes over land is limited for reasons discussed in Byrne and OGorman (2015). Another pair of mechanisms also result in the enhancement of contrast between wet and dry regions. The “upped-ante” mechanism predicts drying over marginally wet regions (Neelin et al., 2003). Warmer free troposphere raises the “ante” for convection and moisture in the wet regions will have to increase to maintain positive convective available potential energy (CAPE), while moisture in the dry regions is unable to increase by the same amount. The enhanced moisture gradients between wet and dry regions superimposed on the climatological advection from dry to wet regions thus causes a negative moisture anomaly in between. The marginally convecting regions then fail to reach the “upped-ante” for convection and therefore dry with warming. At the same time, the “rich-get-richer” mechanism predicts reduction in the gross moist stability (GMS) due to increased boundary-layer moisture and thus enhanced convection in the wet regions (Chou & Neelin, 2004), whereas tropospheric warming and deepening of convection may negate the effect of the “rich-get-richer” mechanism in some cases (Chou et al., 2009).

Common to the previous mechanisms is the decomposition of rainfall changes into moisture changes and circulation changes (thermodynamic changes and dynamic changes), as the long-term mean rainfall can be regarded as the large-scale circulation lifting and condensing the boundary-layer moisture. Such decomposition is also adapted in idealized models for tropical rainfall distribution (Pendergrass & Gerber, 2016). While the moisture changes (thermodynamic change) by 7%/K are robust in observations and climate models (Santer et al., 2007; Willett et al., 2007), inline with the aforementioned constant relative humidity assumption, the circulation changes have more significant uncertainty (Pfahl et al., 2017) especially on regional scales and relatively short monthly timescales (Chadwick et al., 2013; Byrne & OGorman, 2015, which precludes the aforementioned mechanisms from quantitatively explaining the robust increase in the unevenness of tropical rainfall.

In the following, we present a mechanism that makes no assumption about the circulation changes. We show that the unevenness of tropical rainfall is closely related to the frequency distribution of subcloud moist static energy (MSE) and that the changes in the subcloud MSE distribution can be accurately captured by a simple scaling assuming constant relative humidity and uniform warming.

2. Overview of the Mechanism in This Work

A simple picture of the tropical atmosphere goes that the tropical free tropospheric temperature is roughly uniform in the horizontal and follows a moist adiabat in the vertical, which is determined by the subcloud MSE (defined as $c_p T + Lq + gz$, where the three terms represent sensible heat, latent heat, and geopotential respectively, and $c_p = 1,005 \text{ J/kg/K}$ is the heat capacity of dry air, $L = 2.5 \times 10^6 \text{ J/kg}$ is the latent heat in the convective regions (Bretherton & Smolarkiewicz, 1989; Emanuel et al., 1994). The rest of the tropics

have lower subcloud MSE than the convective regions and are stable to deep convection. The unevenness of the tropical rainfall distribution should be related to the distribution of the subcloud MSEs. Heuristically, if the subcloud MSE everywhere increases by the same amount, the unevenness of rainfall should be largely unchanged. On the other hand, if the highest subcloud MSEs for some reason increase faster than the rest, the free troposphere will warm up at a pace that the lower subcloud MSEs (in the nonconvective regions) cannot keep up with. Therefore, dry regions will become more stably stratified, and convection has to concentrate to wet regions with warming resulting in the increasing unevenness of rainfall. With global warming, the differential increase in MSE is a result of the nonlinearity of the Clausius-Clapeyron relationship meaning that saturation vapor pressures increase more for higher climatological temperatures, assuming uniform warming and relatively unchanged relative humidity. Since convective regions are generally warmer and contain more moisture than the nonconvective regions, the same amount of warming will induce more increase in moisture in the wet regions than in the dry regions.

The above mechanism bears some similarity with the “upped-ante” mechanism but is essentially different in several ways. First, although the “upped-ante” mechanism also recognizes the role of free tropospheric temperature in setting the convective “ante,” the changes in the free tropospheric temperature are externally determined: In the El Niño case it is due to teleconnection from neighboring Pacific, while in the global warming case it is due to absorption of infrared radiation (Neelin et al., 2003). Therefore, the “upped-ante” mechanism is only able to address local rainfall changes but is unable to tell whether a reduction in one place could be compensated by an increase in another. Here we argue that the free tropospheric temperature is endogenously determined by the highest subcloud MSE in the tropics rather than local factors or radiation. Therefore, we are able to propose a closed theory for the distribution of rainfall within the entire tropics. Second, the “upped-ante” mechanism also mentions increasing moisture gradients with warming, yet the reason of which hinges on different moisture budgets in wet and dry regions. Here we give a general explanation that applies to both wet and dry regions making use of the assumption of constant relative humidity.

3. Methods and Data

3.1. Metrics for Rainfall and Subcloud MSE Distribution

We use the Gini index, an economic index for inequality of income, as a single-value measurement for the unevenness (Pendergrass & Knutti, 2018) of rainfall distribution in space. The Gini index has been used by Rajah et al. (2014) to study the temporal distribution of rainfall before. Monthly mean rainfall intensities between 30° S and 30° N are sorted in ascending order then accumulated against area. As illustrated in Figure 1a, the Gini index is proportional to the area between the 1:1 line and the cumulative rainfall fraction as a function of cumulative area fraction. The Gini index ranges from 0 to 100, with 0 being completely even and 100 being extremely uneven. An increase in the Gini index is an increase in the unevenness and is associated with a decrease in the area of active convection. Compared to previous metrics for rainfall unevenness that usually bisect the full distribution at arbitrary thresholds, the advantage of the Gini index is that it integrates the entire distribution of rainfall. The Gini index does capture the enhanced contrast between wet and dry regions with warming as previous metrics do (Figure S1 in the supporting information).

We use the relative convective MSE, the difference between the convective MSE and the tropical mean MSE, as a measurement of the shape of the subcloud MSE distribution (Figure 1b):

$$\text{Relative convective MSE} = \text{Convective subcloud MSE} - \text{Mean subcloud MSE}. \quad (1)$$

Convective MSE is defined as the rainfall-weighted mean of subcloud MSE treating rainfall as a proxy for convection intensity (Flannaghan et al., 2014). Since the atmosphere is only unstable to convection when subcloud MSE is high, the convective MSE is essentially a weighted mean of the highest subcloud MSE values. The relative convective MSE thus captures how close the entire distribution of tropical subcloud MSE is to convective instability.

3.2. Data

We first use observations and reanalysis to support the proposed mechanism, and then use global climate model simulations to understand future projections. Rainfall observations from Tropical Rainfall Measuring

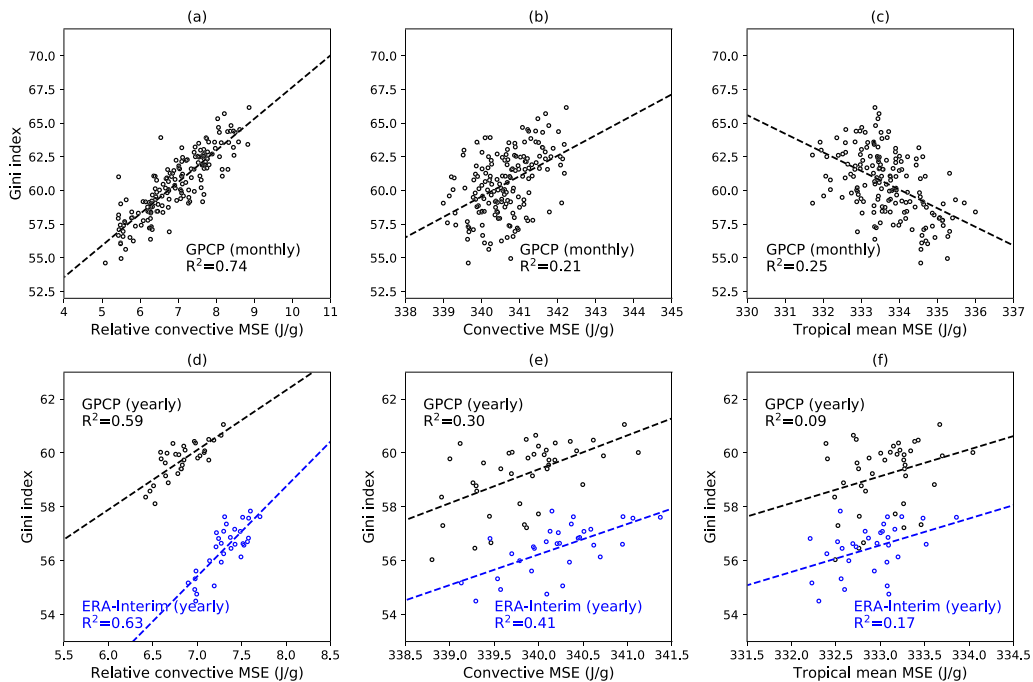


Figure 2. Gini index versus relative convective MSE, convective MSE, and tropical mean MSE. Each point in (a)–(c) is a month from January 2001 to December 2014. Each point in (d)–(f) is a year from 1988 to 2018.

Mission (TRMM) (Huffman et al., 2007) on $0.25^\circ \times 0.25^\circ$ grid and Global Precipitation Climatology Project (GPCP) (Huffman et al., 2001) on $1^\circ \times 1^\circ$ or $2.5^\circ \times 2.5^\circ$ grid and rainfall reanalysis from European Centre for Medium-Range Weather Forecasts reanalyses (ERA-Interim)(Dee et al., 2011) on $0.75^\circ \times 0.75^\circ$ grid are used. When matching a precipitation data set to the subcloud MSE field based on ERA-Interim, the higher-resolution data set is interpolated to the grid of the lower-resolution data set conserving total flux for rainfall, or bilinearly for MSE. For GPCP we only use data from year 1988 on for data consistency. The microwave ocean measurements from the Special Sensor Microwave Imager (SSM/I) have been added to the blend of satellite infrared radiances and rain gauges since 1988. Inconsistency in the Gini index of tropical rainfall before and after 1988 is observed which is likely a result of adding new instruments. MSE is derived from monthly mean ERA-Interim reanalysis field, and subcloud MSE is the average of MSE between 924.9 and 1,000.1 hPa following Williams et al. (2009),Williams and Pierrehumbert (2017). For the global warming simulations, we analyze monthly mean rainfall and diagnosed subcloud MSE with global climate models from the Coupled Model Intercomparison Project phase 5 (CMIP5) (Taylor et al., 2012) in the idealized CO_2 increase experiment (increasing CO_2 by 1% per year for 140 years until quadrupling). Simulations forced with emissions following the RCP 8.5 scenario yield similar results. To overcome the sparseness of output vertical levels in the subcloud layer (only 925 and 1,000 hPa) and lack of land information on 1,000 hPa in most models, we calculated the subcloud MSE as the average of near-surface MSE and 925-hPa MSE.

4. Results

4.1. Gini Index With Relative Convective MSE

In this section, we will show the correspondence between the relative convective MSE (convective MSE minus the tropical mean MSE) defined in the previous section and the Gini index of rainfall on multiple time scales in both observations/reanalysis and climate models. However, in the rest of the paper, we will focus on the yearly time scale for the purpose of understanding long-term trends.

In the observations and the reanalysis data, the explained month-to-month variability is 77% for TRMM rainfall and 74% for GPCP rainfall for all months from 2001 to 2014 (Figure 2a), and the explained interannual variability is 63% for ERA-Interim rainfall and 59% for GPCP rainfall from 1988 to 2018 (Figure 2d). The explained interannual variability in TRMM rainfall is only 32% (not shown), which could be a result of short record length. It is worth noticing that the monthly data shown in Figure 2a are not deseasonalized. While this demonstrates that the proposed mechanism works for all seasons in general, there is the caveat that the

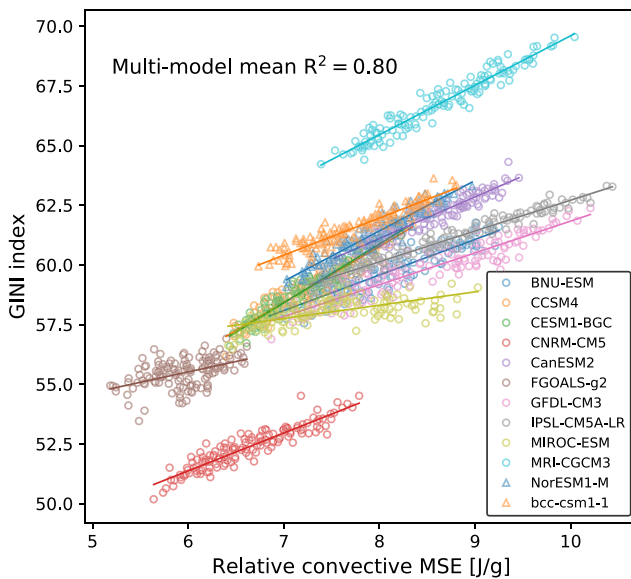


Figure 3. Gini index versus relative convective MSE of each CMIP5 model in the idealized CO₂ increase experiment. Each marker is a year. Selected models from different modeling centers are shown.

high correlation is due to the strong seasonality of both variables rather than any causality. However, the fact that the two components of relative convective MSE (convective MSE and the tropical mean MSE) are not correlated with the Gini index even though they exhibit strong seasonality (Figures 2b and 2c) provides further support, and the same applies to the interannual variability (Figures 2e and 2f). Therefore, the high correlation between the Gini index and the relative convective MSE shown in Figures 2a and 2d is very likely a result of the mechanism proposed in section 2. This tight relationship only emerges on time scale longer than a month, whereas on a daily time scale, the relationship is loosened by stochastic processes, and the correlation coefficient is much less (Figure S2).

In CMIP5 models, the tight relationship between the annual-mean Gini index and the relative convective MSE also applies. The unevenness of rainfall increases in 26 out of the 28 models examined here, indicated by the increased Gini index at the end of the simulation (Table S1). Relative convective MSE explains on average about 80% of variability in the annual-mean Gini index in all models (Figure 3). The R^2 values for all models are shown in Table S1, where 21 out of 27 models has R^2 values of higher than 0.85, though 4 models show R^2 values of below 0.41. Up to this point, we can conclude that the robust increasing rainfall unevenness across models can be explained by the robust increase in the relative convective MSE, which is going to be understood with a simple scaling in the following section.

4.2. Insight for Increase in Relative Convective MSE With Global Warming

Figure 4 shows the subcloud MSE distribution in the present climate (first 10 years of simulation) and in a warmer climate (last 10 years of simulation) averaged over all models. In addition to a shift of the entire distribution to higher MSE values with warming, the shape of the distribution has also changed. The high end of the distribution has increased more in MSE than the low end, resulting in the broadening of the distribution in MSE space. Since the convective subcloud MSE is a weighted mean of the highest subcloud MSE values (Figure 1b), the relative convective MSE increases faster than the tropical mean with warming.

The change in the distribution of subcloud MSE can be explained by a uniform temperature increase. We predict the distribution in the last 10 years of the simulation by perturbing the subcloud MSE in the first 10 years. For each location and month, subcloud MSE is perturbed by the amount Δh defined as follows:

$$\Delta h = c_p \Delta \bar{T} + L_v q \alpha \Delta \bar{T}, \quad (2)$$

where $\Delta \bar{T}$ is the change in tropical mean temperature; $\alpha = 7\text{%/K}$, which is approximately the rate at which saturation vapor pressure increases with temperature according to the Clausius-Clapeyron relationship; and

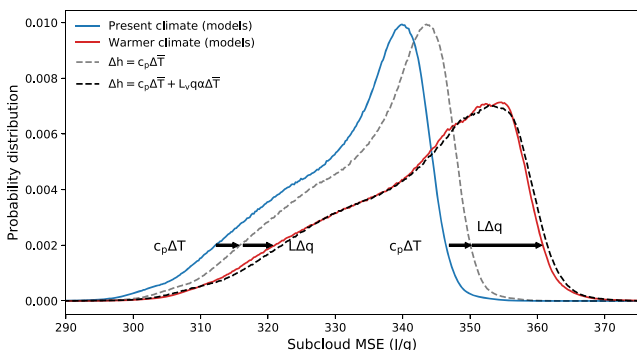


Figure 4. Multimodel-mean subcloud MSE distribution in the first (solid blue) and last (solid red) 10 years of the simulation and the predicted distribution from perturbation of the first 10 years (dashed black line). The dashed gray line shows the effect of temperature change only.

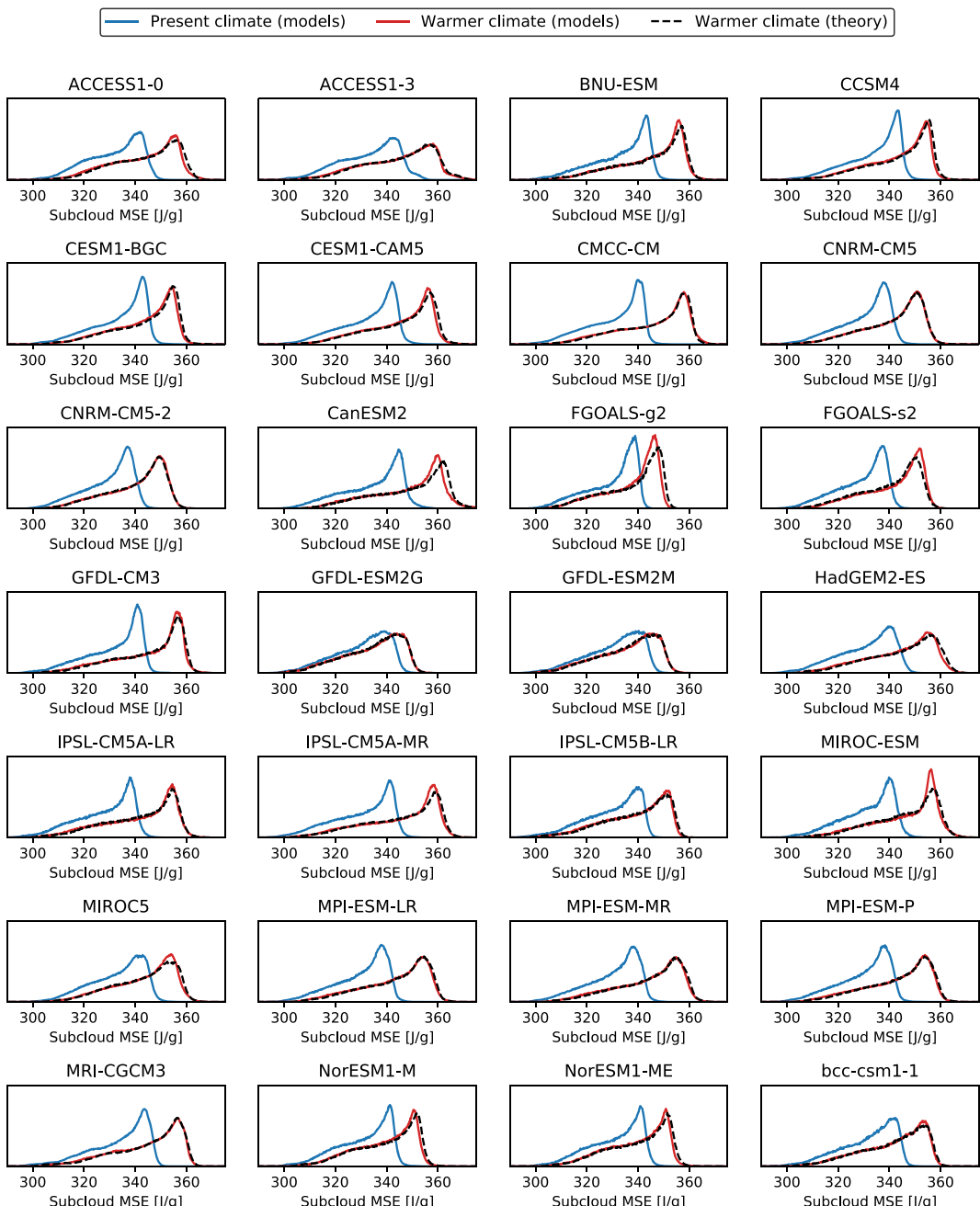


Figure 5. Subcloud MSE distribution in the first and last 10 years of the simulation and the predicted distribution from perturbation of the first 10 years (dashed black lines) for each model. Labels of Y axis should be “probability distribution” as in Figure 4 and are omitted here.

q is the specific humidity. The Δh prediction in equation (2) only uses local information for the specific humidity q and the tropical mean temperature change (\bar{T}). In a nutshell, this scaling assumes unchanged relative humidities with warming and uniform warming (The “uniform” here means a shift in temperature histogram, which does not necessarily mean spatially uniform warming. A uniform shift in temperature histogram and a reshuffle of temperatures in space can result in spatially nonuniform warming).

Despite the crudeness, the scaling captures the shift and the shape change of subcloud MSE very accurately not only in the multimodel mean (Figure 4) but also in each model (Figure 5.). The change in the relative convective MSE by the end of the simulation for each model can be predicted by the difference between

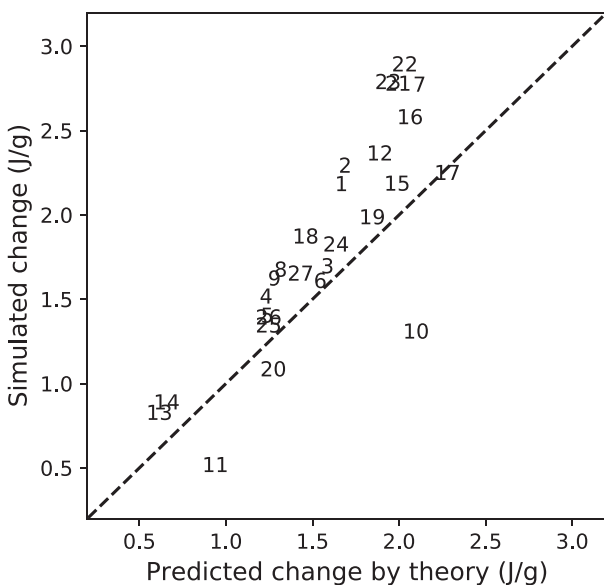


Figure 6. Simulated change in the relative convective MSE for each model versus the predicted change by theory. The corresponding model for each number is listed in Table S1.

Acknowledgments

This report was prepared by Y. Z. under award NA18OAR4320123 from the National Oceanic and Atmospheric Administration, U.S. Department of Commerce. The statements, findings, conclusions, and recommendations are those of the author(s) and do not necessarily reflect the views of the National Oceanic and Atmospheric Administration, or the U.S. Department of Commerce. S. F. acknowledges support from National Science Foundation Awards AGS-1417659 and AGS-1743753. ERA-Interim data provided by European Centre for Medium-range Weather Forecast (ECMWF) can be accessed online (at <https://www.ecmwf.int/en/forecasts/datasets/archive-datasets/reanalysisdatasets/era-interim>). Tropical Rainfall Measuring Mission (TRMM) data provided by NASA can be accessed at the GES DISC website (<https://disc.gsfc.nasa.gov/datasets/TRMM&urluscore;3B43&urluscore;7/> summary). Global Precipitation Climatology Project (GPCP) data provided by NASA can be accessed online (at <ftp://meso.gsfc.nasa.gov/pub/1dd-v1.2>). CMIP5 model data provided by the World Climate Research Programme's Working Group on Coupled Modelling and climate modeling groups can be accessed at the ESGF-LLNL website (<https://esgf-node.llnl.gov/projects/cmip5>).

moisture in the convective regions (\hat{q} ; rainfall-weighted moisture) and tropical mean moisture (\bar{q}) given the tropical mean warming ($\Delta\bar{T}$) by the end of the simulation following Clausius-Clapeyron relation (combining equations (1) and (2)):

$$\Delta(\text{Relative convective MSE}) = \alpha\Delta\bar{T}L_v(\hat{q} - \bar{q}). \quad (3)$$

Figure 6 shows that equation (3) captures the intermodel scatter of simulated changes in the relative convective MSE. Models with larger moisture gradients in the base state undergo larger relative convective MSE change. The predicted changes are somewhat biased, which is not surprising given the simplicity of equation (2). Specifically, equation (2) does not take into account that relative humidity tends to weakly increase over the ocean and decrease over the land (Boer, 1993), and the warming is not spatially uniform.

5. Conclusion

We have shown that the increasing unevenness of tropical rainfall with global warming can be understood as a result that the Clausius-Clapeyron relationship amplifying the moist static energy (MSE) gradients in the subcloud layer. There are two essential links in this chain of reasoning: (i) The unevenness of the monthly rainfall in both observations and models (measured by the Gini index) is well explained by the relative convective MSE, which is a bulk metric of how high the highest subcloud MSE is compared to the tropical mean. (ii) The simulated changes in the relative convective MSE with global warming can be very well captured by the subcloud MSE changes associated with uniform warming and fixed relative humidity.

Our argument relates to previously published concept of SST threshold for convection (Palmen, 1948), whereby the invariant shape of SST distribution with warming implies constant convective area since the SST threshold warms as much as the mean SST (Johnson & Xie, 2010; Williams et al., 2009). Our work stresses that even uniform SST warming leads to a decrease in convective area fraction as a consequence of the Clausius-Clapeyron scaling of subcloud MSE, irrespective of whatever changes that may occur in the large-scale circulation.

References

- Allan, R. P., Soden, B. J., John, V. O., Ingram, W., & Good, P. (2010). Current changes in tropical precipitation. *Environmental Research Letters*, 5(2), 025205. <https://doi.org/10.1088/1748-9326/5/2/025205>
- Boer, G. J. (1993). Climate change and the regulation of the surface moisture and energy budgets. *Climate Dynamics*, 8(5), 225–239. <https://doi.org/10.1007/BF00198617>
- Bretherton, C. S., & Smolarkiewicz, P. K. (1989). Gravity waves, compensating subsidence and detrainment around cumulus clouds. *Journal of the Atmospheric Sciences*, 46(6), 740–759. [https://doi.org/10.1175/1520-0469\(1989\)046<0740:GWCSAD>2.0.CO;2](https://doi.org/10.1175/1520-0469(1989)046<0740:GWCSAD>2.0.CO;2)
- Byrne, M. P., & OGorman, P. A. (2015). The response of precipitation minus evapotranspiration to climate warming: Why the wet-get-wetter, dry-get-drier scaling does not hold over land. *Journal of Climate*, 28(20), 8078–8092. <https://doi.org/10.1175/JCLI-D-15-0369.1>
- Chadwick, R., Boulle, I., & Martin, G. (2013). Spatial patterns of precipitation change in cmip5: Why the rich do not get richer in the tropics. *Journal of Climate*, 26(11), 3803–3822. <https://doi.org/10.1175/JCLI-D-12-00543.1>
- Chou, C., Chiang, J. C., Lan, C.-W., Chung, C.-H., Liao, Y.-C., & Lee, C.-J. (2013). Increase in the range between wet and dry season precipitation. *Nature Geoscience*, 6(4), 263–267. <https://doi.org/10.1038/ngeo1744>
- Chou, C., & Lan, C.-W. (2012). Changes in the annual range of precipitation under global warming. *Journal of Climate*, 25(1), 222–235. <https://doi.org/10.1175/JCLI-D-11-00097.1>
- Chou, C., & Neelin, J. D. (2004). Mechanisms of global warming impacts on regional tropical precipitation. *Journal of Climate*, 17(13), 2688–2701. [https://doi.org/10.1175/1520-0442\(2004\)017<2688:MOGWIO>2.0.CO;2](https://doi.org/10.1175/1520-0442(2004)017<2688:MOGWIO>2.0.CO;2)
- Chou, C., Neelin, J. D., Chen, C.-A., & Tu, J.-Y. (2009). Evaluating the rich-getricher mechanism in tropical precipitation change under global warming. *Journal of Climate*, 22(8), 1982–2005. <https://doi.org/10.1175/2008JCLI2471.1>
- Dee, D. P., Uppala, S., Simmons, A., Berrisford, P., Poli, P., & Kobayashi, S. (2011). The era-interim reanalysis: Configuration and performance of the data assimilation system. *Quarterly Journal of the Royal Meteorological Society*, 137(656), 553–597. <https://doi.org/10.1002/qj.828>
- Emanuel, K., Neelin, J., & Bretherton, C. (1994). On large-scale circulations in convecting atmospheres. *Quarterly Journal of the Royal Meteorological Society*, 120(519), 1111–1143. <https://doi.org/10.1002/qj.4971205190>
- Flannagan, T. J., Fueglistaler, S., Held, I. M., Po-Chedley, S., Wyman, B., & Zhao, M. (2014). Tropical temperature trends in Atmospheric General Circulation Model simulations and the impact of uncertainties in observed SSTs. *Journal of Geophysical Research: Atmospheres*, 119, 13,327–13,337. <https://doi.org/10.1002/2014JD022365>

- Giorgi, F., Im, E.-S., Coppola, E., Diffenbaugh, N., Gao, X., Mariotti, L., & Shi, Y. (2011). Higher hydroclimatic intensity with global warming. *Journal of Climate*, 24(20), 5309–5324.
- Gu, G., & Adler, R. F. (2018). Precipitation intensity changes in the tropics from observations and models. *Journal of Climate*, 31(12), 4775–4790. <https://doi.org/10.1175/JCLI-D-17-0550.1>
- Held, I. M., & Soden, B. J. (2000). Water vapor feedback and global warming. *Annual Review of Energy and the Environment*, 25(1), 441–475. <https://doi.org/10.1146/annurev.energy.25.1.441>
- Held, I. M., & Soden, B. J. (2006). Robust responses of the hydrological cycle to global warming. *Journal of Climate*, 24(5), 1559–1560. <https://doi.org/10.1175/2010JCLI4045.1>
- Huffman, G. J., Adler, R. F., Morrissey, M. M., Bolvin, D. T., Curtis, S., Joyce, R., & Susskind, J. (2001). Global precipitation at one-degree daily resolution from multisatellite observations. *Journal of Hydrometeorology*, 2(1), 36–50. [https://doi.org/10.1175/1525-7541\(2001\)002<0036:GPAODD>2.0.CO;2](https://doi.org/10.1175/1525-7541(2001)002<0036:GPAODD>2.0.CO;2)
- Huffman, G. J., Bolvin, D. T., Nelkin, E. J., Wolff, D. B., Adler, R. F., Gu, G., & Stocker, E. F. (2007). The trmm multisatellite precipitation analysis (tmpa): Quasi-global, multiyear, combined-sensor precipitation estimates at fine scales. *Journal of Hydrometeorology*, 8(1), 38–55. <https://doi.org/10.1175/JHM560.1>
- Johnson, N. C., & Xie, S.-P. (2010). Changes in the sea surface temperature threshold for tropical convection. *Nature Geoscience*, 3(12), 842–845. <https://doi.org/10.1038/ngeo1008>
- Lintner, B. R., Biasutti, M., Diffenbaugh, N. S., Lee, J.-E., Niznik, M. J., & Findell, K. L. (2012). Amplification of wet and dry month occurrence over tropical land regions in response to global warming. *Journal of Geophysical Research-Atmospheres*, 117(D11). <https://doi.org/10.1029/2012JD017499>
- Liu, C., & Allan, R. P. (2013). Observed and simulated precipitation responses in wet and dry regions 1850–2100. *Environmental Research Letters*, 8(3), 034002. <https://doi.org/10.1088/1748-9326/8/3/034002>
- Neelin, J., Chou, C., & Su, H. (2003). Tropical drought regions in global warming and El Niño teleconnections. *Geophysical Research Letters*, 30(24). <https://doi.org/10.1029/2003GL018625>
- Palmen, E. (1948). On the formation and structure of tropical hurricanes. *Geophysica*, 3(1), 26–38.
- Pendergrass, A. G., & Gerber, E. P. (2016). The rain is askew: Two idealized models relating vertical velocity and precipitation distributions in a warming world. *Journal of Climate*, 29(18), 6445–6462. <https://doi.org/10.1175/JCLI-D-16-0097.1>
- Pendergrass, A. G., & Knutti, R. (2018). The uneven nature of daily precipitation and its change. *Geophysical Research Letters*, 45, 11,980–11,988. <https://doi.org/10.1029/2018GL080298>
- Pfahl, S., OGorman, P. A., & Fischer, E. M. (2017). Understanding the regional pattern of projected future changes in extreme precipitation. *Nature Climate Change*, 7(6), 423–427. <https://doi.org/10.1038/nclimate3287>
- Polson, D., & Hegerl, G. (2017). Strengthening contrast between precipitation in tropical wet and dry regions. *Geophysical Research Letters*, 44, 365–373. <https://doi.org/10.1002/2016GL071194>
- Polson, D., Hegerl, G., Allan, R., & Sarojini, B. B. (2013). Have greenhouse gases intensified the contrast between wet and dry regions? *Geophysical Research Letters*, 40, 4783–4787. <https://doi.org/10.1002/grl.50923>
- Rajah, K., O'Leary, T., Turner, A., Petrakis, G., Leonard, M., & Westra, S. (2014). Changes to the temporal distribution of daily precipitation. *Geophysical Research Letters*, 41, 8887–8894. <https://doi.org/10.1002/2014GL062156>
- Santer, B. D., Mears, C., Wentz, F., Taylor, K., Gleckler, P., & Wigley, T. (2007). Identification of human-induced changes in atmospheric moisture content. *Proceedings of the National Academy of Sciences*, 104(39), 15,248–15,253. <https://doi.org/10.1073/pnas.0702872104>
- Taylor, K. E., Stouffer, R. J., & Meehl, G. A. (2012). An overview of cmip5 and the experiment design. *Bulletin of the American Meteorological Society*, 93(4), 485–498. <https://doi.org/10.1175/BAMS-D-11-00094.1>
- Willett, K. M., Gillett, N. P., Jones, P. D., & Thorne, P. W. (2007). Attribution of observed surface humidity changes to human influence. *Nature*, 449(7163), 710–712. <https://doi.org/10.1038/nature06207>
- Williams, I. N., & Pierrehumbert, R. T. (2017). Observational evidence against strongly stabilizing tropical cloud feedbacks. *Geophysical Research Letters*, 44, 1503–1510. <https://doi.org/10.1002/2016GL072202>
- Williams, I. N., Pierrehumbert, R. T., & Huber, M. (2009). Global warming, convective threshold and false thermostats. *Geophysical Research Letters*, 36, L21805. <https://doi.org/10.1029/2009GL039849>

Erratum

In the originally published version of this article, Pendergrass and Knutti (2018) was not cited in the methods section and the images in the supporting information did not appear correctly. The reference has been included and cited, the supporting information has been updated, and the present version may be considered the authoritative version of record.